Composition and Structure of Whey Protein/Gum Arabic Coacervates

ARTICLE *in* BIOMACROMOLECULES · JULY 2004

Impact Factor: 5.75 · DOI: 10.1021/bm049970v · Source: PubMed

3 AUTHORS, INCLUDING:

R. Hans Tromp
NIZO food research
59 PUBLICATIONS **1,275** CITATIONS
SEE PROFILE

C.G. (Kees) De Kruif
Utrecht University
243 PUBLICATIONS **10,524** CITATIONS
SEE PROFILE

CHAPTER 5

Composition and Structure of Whey Protein / Gum Arabic Coacervates*

ABSTRACT

Complex coacervation in whey protein / gum arabic (WP/GA) mixtures was studied as a function of three main key parameters: pH, initial protein to polysaccharide mixing ratio $(Pr:Ps)_{ini}$, and ionic strength. Previous studies had already revealed under which conditions a coacervate phase was obtained. This study aimed now to understand how these parameters influence the phase separation kinetics, the coacervate composition and the internal coacervate structure. At a defined $(Pr:Ps)_{ini}$, an optimum pH of complex coacervation was found (pH_{opt}), at which the strength of electrostatic interaction was maximum. For $(Pr:Ps)_{ini}$ = 2:1, the phase separation occurred the fastest and the final coacervate volume was the largest at pH_{opt} = 4.0. The composition of the coacervate phase was determined after 48 h of phase separation and revealed that, at pH_{opt}, the coacervate phase was the most concentrated. Varying the $(Pr:Ps)_{ini}$ shifted the pH_{opt} to higher values when $(Pr:Ps)_{ini}$ was increased, and to lower values when $(Pr:Ps)_{ini}$ was decreased. This phenomenon was due to the level of charge compensation of the WP/GA complexes. Finally, the structure of the coacervate phase was studied with small angle X-ray scattering (SAXS). SAXS data confirmed that at pH_{opt} the coacervate phase was dense and structured. Model calculations revealed that the structure factor of WP induced a peak at Q = 0.7 nm^{-1}, illustrating that the coacervate phase was more structured, inducing the stronger correlation length of WP molecules. When the pH was changed to more acidic values, the correlation peak faded away, due to a more open structure of the coacervate. A shoulder in the scattering pattern of the coacervates was visible at small Q. This peak was attributed to the presence of residual charges on the GA. The peak intensity was reduced when the strength of interaction was increased, highlighting a greater charge compensation of the polyelectrolyte. Finally, increasing the ionic strength led to a less concentrated, a more heterogeneous, and a less structured coacervate phase, induced by the screening of the electrostatic interactions.

*F. Weinbreck, R. H. Tromp, C. G. de Kruif,
Considered for publication in *Biomacromolecules*

INTRODUCTION

For application of biopolymers (such as proteins and polysaccharides) in the pharmaceutical, cosmetic, and food industries, their interactions are of major relevance in their respective applications. The repulsive and attractive forces between the biopolymers underlie two different phenomena: biopolymer incompatibility and complex formation [Tolstoguzov, 2003]. Complex coacervation is a specific type of complex formation. It is the phase separation which occurs in a mixture of oppositely charged polymer solutions. Insoluble complexes between the polymers are formed and they concentrate in liquid droplets, also called coacervate droplets. The coacervate droplets sediment and fuse to form a coacervate phase. Thus, complex coacervation leads to the formation of two liquid phases: the upper phase, poor in polymers and rich in solvent, and a lower coacervate phase concentrated in polymers [Bungenberg de Jong, 1949a]. Biopolymer coacervates are used as fat replacers or meat analogues, for coatings and for encapsulation of flavors or drugs, and in biomaterials (*e.g*. edible films and packaging) [Bakker *et al.*, 1994; Burgess, 1994; Luzzi, 1970; Kester and Fennema, 1986].

Most of the studies on complex coacervation have been carried out on the gelatin / gum arabic system, since the pioneering work of Bungenberg de Jong (1949a). The formation of biopolymer complexes arises mainly from electrostatic interactions and is dependent on the ionization degree of the polymers, and thus the pH. The presence of salt can suppress complex coacervation to varying degrees, depending on the nature and concentration of salt [Bungenberg de Jong, 1949a; Overbeek and Voorn, 1957; Schmitt *et al.*, 1998]. The biopolymer concentration is also a critical parameter, and an optimum mixing ratio exists which corresponds to an electrically equivalent amount of each polymer [Burgess and Carless, 1984]. The trend is nowadays to replace gelatin by another protein; that is why whey protein (WP) and gum arabic (GA) were used in the present study. The WP used was a whey protein isolate consisting of 75% â-lactoglobulin (â-lg), which is the main protein responsible for the complex formation with GA [Weinbreck *et al.*, 2003a]. Native â-lg has an iso-electric point (pI) of 5.2 and is thus positively charged below this pI value. Commercial samples of WP always contained some denatured â-lg, which drastically influences the coacervation [Schmitt *et al.*, 2000a; Sanchez and Renard, 2002c]; therefore in this study aggregates of denatured â-lg were removed. GA is a complex polysaccharide exuded from the

African tree *Acacia senegal*. It is an arabinogalactan composed of three distinct fractions with different protein contents and different molecular weights [Osman *et al.*, 1993; Randall *et al.*, 1989]. The composition analysis of GA revealed the presence of a main galactan chain carrying heavily branched galactose/arabinose side chains. The carbohydrate moiety is composed of D-galactose (40% of the residues), L-arabinose (24%), L-rhamnose (13%), and two uronic acids, responsible for the polyanionic character of the gum, D-glucuronic acid (21%) and 4-O-methyl-D-glucuronic acid (2%). The structure of GA is complex and poorly known. GA is negatively charged above pH 2.2, since at low pH (< 2.2) the dissociation of the carboxyl groups is suppressed. GA displays good emulsifying properties and its viscosity is low compared to other polysaccharides of similar molar mass [Sanchez *et al.*, 2002b].

Previous work was carried out on the complex formation of WP and GA as a function of key parameters, such as pH, ionic strength, biopolymer concentration and initial protein to polysaccharide mixing ratio $(Pr:Ps)_{ini}$ [Weinbreck *et al.*, 2003a; Schmitt *et al.*, 1999; Weinbreck and de Kruif, 2003b]. Weinbreck *et al.* (2003a) demonstrated that around the iso-electric point of the WP, soluble complexes of WP/GA were formed (at pH_c), and if the pH was decreased even further (< $pH_{\phi 1}$), complexes associated and phase separated into a coacervate phase. At even lower pH (< $pH_{\phi 2}$), GA became neutral and complex coacervation was prevented. The pH window where complex coacervation occurred shrank with increasing ionic strength due to the screening of the charges by the microions. The structure of the primary soluble WP/GA complexes was proposed to be a GA molecule decorated with WP. Secondary aggregation of the primary soluble WP/GA complexes was scarcely studied and the final microstructure of the coacervate phase remains unknown so far. There is a need to study the structure of coacervating systems [Turgeon *et al.*, 2003]. Studies on synthetic polyelectrolytes reported a sponge-like and hierarchically self-assembled “fractal” network of coacervates as found from electron microscopy [Menger *et al.*, 2000; Menger, 2002]. Recently, Leisner *et al.* (2003) investigated the structure of a poly(glutamic acid) / dendrimer coacervate by light scattering and small-angle X-ray scattering. A first attempt to describe the kinetics of complex coacervation was made with â-lg / GA using diffusing wave spectroscopy (DWS) and confocal scanning laser microscopy (CSLM) [Schmitt *et al.*, 2001a]. Depending on the initial mixing ratio, the DWS patterns were rather complex, combining both coalescence of the particles and sedimentation. Sanchez *et al.* (2002a) continued the study of the phase separation of â-lg / GA mixtures with CSLM and small angle

static light scattering, and they concluded that the aggregation of coacervates leads to the formation of an equilibrated heterogeneous structure whose interfaces were rough. The authors could not describe the phase separation mechanism on the basis of spinodal decomposition or nucleation and growth since the initial stages were too fast to be measured. So far, studies on the structure of equilibrated biopolymer coacervates are still lacking. Since the conditions for WP/GA coacervate formation were known, in this work phase separation *per se* was studied as a function of the key parameters: pH, ionic strength and Pr:Ps ratio. The first goal of this study was to analyze the kinetics of phase separation and the growth of the coacervate phase by determining which parameters influence the sedimentation kinetics and by relating them to the composition of the coacervate phase. Indeed, the coacervate phases were characterized (water content and biopolymer content) as a function of pH, ionic strength and $(Pr:Ps)_{ini}$ ratio. And finally, the internal structure of the coacervate was studied by small angle X-ray scattering (SAXS) in the conditions previously used.

EXPERIMENTAL SECTION

Materials

Bipro from Davisco Foods International (Le Sueur, USA) is an isolate of whey protein (WP) consisting mainly of â-lactoglobulin (â-lg), and á-lactalbumin (á–la). Residual whey protein aggregates were removed by acidification (at pH 4.75) and centrifugation (1 h at 33000 rpm with a Beckman L8-70M ultracentrifuge, Beckman Instruments, The Netherlands). The supernatant was then freeze-dried (in a Modulo 4K freeze-dryer from Edwards High Vacuum International, UK). Finally, the resulting powder was stored at 5°C. The final powder contained (w/w) 88.1% protein (N x 6.38), 9.89% moisture, 0.3% fat and 1.84% ash (0.66% Na^+, 0.075% K^+, 0.0086% Mg^{2+}, and 0.094 % Ca^{2+}). The protein content of the treated Bipro was: 14.9% á-la, 1.5% BSA, 74.9% β-lg, and 3.2% immunoglobulin (IMG).

Gum arabic (GA; IRX 40693) was a gift from Colloides Naturels International (Rouen, France). The powder contained (w/w) 90.17% dry solid, 3.44% moisture, 0.338% nitrogen and 3.39% ash (0.044% Na^+, 0.76% K^+, 0.20% Mg^{2+} and 0.666% Ca^{2+}). Its weight average molar mass (M_w = 520 000 g/mol) and its average radius of gyration (R_g = 24.4 nm) were determined by size exclusion chromatography followed by multiangle laser light scattering (SEC MALLS). SEC MALLS was carried out using a TSK-Gel

6000 PW + 5000 PW column (Tosoh Corporation, Tokyo, Japan) in combination with a precolumn Guard PW 11. The separation was carried out at 30°C with 0.1 M $NaNO_3$ as eluent at a flow rate of 1.0 mL min^{-1}.

Stock solutions of 3% (w/w) were prepared by dissolving the powder in deionized water.

The zeta-potential of the 0.1% (w/w) WP and 0.1% (w/w) GA mixtures was measured as a function of pH with a Zetasizer 2000 (Malvern, USA).

Kinetics of phase separation

The stock solutions of 3% (w/w) WP and GA were mixed to obtain a final volume of 30 mL with a defined protein to polysaccharide $(Pr:Ps)_{ini}$ ratio (w/w). The initial pH of the stock solution was 7.0. Sodium azide (0.02% w/w) was added to prevent bacterial growth. At time t_0, the mixtures were acidified using 0.1 M and 1 M HCl to reach the desired pH value (in the range from 3.0 to 5.0). First, the influence of pH at various $(Pr:Ps)_{ini}$ (1:1, 2:1, 8:1) was investigated. Then, the influence of the ionic strength was studied at $(Pr:Ps)_{ini}$ = 2:1 and pH = 4.0. The ionic strength was adjusted with NaCl in the range 0 – 100 mM. After acidification, the samples were directly placed in a graduated tube at 25°C and the coacervate phase volume was measured as a function of time. Measurements were taken every minute at first, and then every day for 7 days. Each kinetics experiment was repeated at least twice.

Composition of the coacervate phase

WP/GA coacervates were prepared as mentioned above at $(Pr:Ps)_{ini}$ of 1:1, 2:1, or 8:1 at various pH values. WP/GA coacervates were also prepared at $(Pr:Ps)_{ini}$ = 2:1, pH 4.0 for [NaCl] ranging from 0 mM to 100 mM. After acidification to the desired pH value, the mixtures were poured into a decanter and left to phase separate for 48 h. Then, the amount of water contained in each coacervate phase (dense lower phase) was determined at least in duplicate by weighing the coacervate phase before and after freeze-drying. The concentrations of residual WP and GA in the upper phase were determined by HPLC. The main proteins of WP (*i. e*. α-la and â-lg) were detected with a UV detector at 280 nm (Applied Biosystems), whereas the GA was detected by refraction index (RI, Erma-7510, Betron Scientific).The injector was a Waters 717 plus Autosampler. A volume of 25 ìl was injected for each run. The column was a Biosep.

Sec. 2000 (Phenomenex) and the pump was a Waters Associates (Isocratisch) with a flow of 0.7 ml/min.

Small angle X-ray scattering (SAXS) measurements

WP/GA coacervates were prepared as described in the paragraph above. Experiments were carried out on the lower coacervate phase. Small angle X-ray scattering (SAXS) measurements were made at the Dutch-Belgian beam-line (DUBBLE) at the European Synchrotron Radiation Facility (ESRF) in Grenoble (France). The cuvettes contained 19.65 mm^3 of sample. The wavelength of the X-rays was λ = 0.93 Å, the detector was a two-dimensional (512 x 512 pixels) gas-filled detector placed at 5 m distance from the sample. The scattering wave vector (Q) was between 0.1 and 1.7 nm^{-1} (corresponding to a range of observable length scales between 62.8 nm and 3.7 nm in real space). The temperature of the samples was kept at 25°C.

RESULTS AND DISCUSSION

Kinetics of phase separation

The study aimed to characterize the influence of various factors such as pH, initial protein to polysaccharide ratio $(Pr:Ps)_{ini}$, and ionic strength, on the complex coacervation of whey proteins (WP) and gum arabic (GA). Coacervation of a WP/GA mixture occurred in a specific pH range [Weinbreck *et al.*, 2003a]. Insoluble complexes of WP and GA concentrated into coacervate droplets that coalesced and accumulated with time at the bottom of a graduated tube [Sanchez *et al.*, 2002a]. The volume of the bottom coacervate layer could thus be measured as a function of time. The phase separation of the complex coacervation process can be divided into several stages. This work aimed to probe the sedimentation kinetics of the coacervate droplets (referred to as phase separation kinetics) by measuring the volume of the coacervate phase as a function of time (from minutes to days). A picture of the system with well separated phases is given in Figure 5.1 (photo A). After phase separation the coacervate phase remained liquid-like (Figure 5.1, photo B).

Mixtures of WP/GA were prepared at various pH values (3.0; 3.5; 3.8; 4.0; 4.2; 4.35; 4.5), the initial volume of each mixture being 30 mL, with a total biopolymer concentration (Cp) of 3% (w/w), a $(Pr:Ps)_{ini}$ of 2:1, and a low ionic strength (no NaCl added). The fraction of the coacervate phase (percentage of total volume) is plotted for

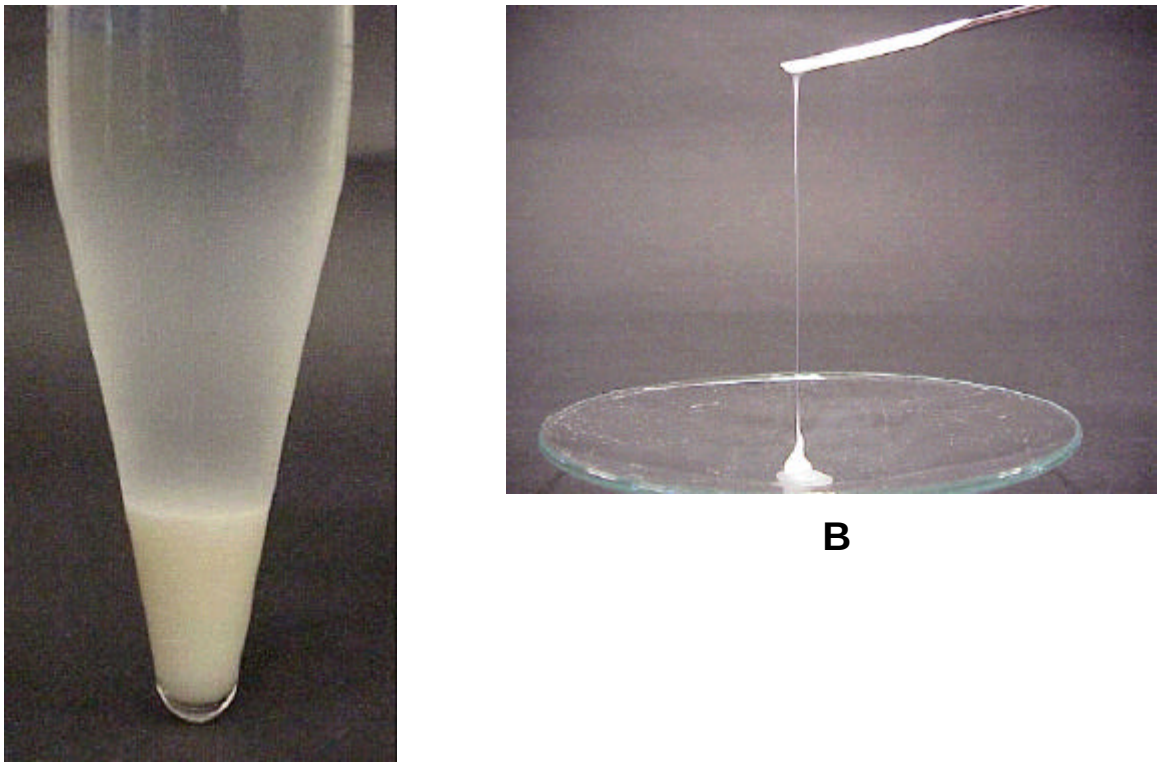

Figure 5.1: Pictures of (A): a phase separated mixture of WP/GA after 1 week of phase separation; the lower phase is the coacervate phase; (B): WP/GA coacervate phase poured with a spatula.

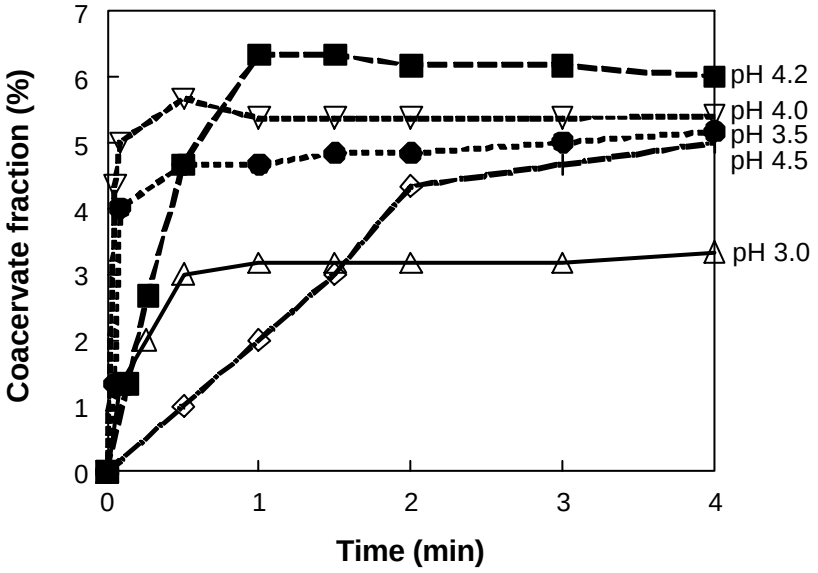

Figure 5.2: Fraction of WP/GA coacervate phase (% of total volume) as a function of time, Cp = 3%, $(Pr:Ps)_{ini}$ = 2:1, [NaCl] = 0 mM. ( ): pH 3.0; ( ): pH 3.5; (∇): pH 4.0; ( ): pH 4.2; ( ): pH 4.5.

various pH values as a function of time in Figure 5.2. The volume of the coacervate phase increased very rapidly during the first 4 min. After 24 h, the volume of the coacervate phase was stable at every pH value, except at pH 4.5, where the volume decreased slightly during 3 days. This phenomenon could be due to a slow rearrangement of the coacervate phase. Indeed, if the charge compensation was not completely achieved (GA in excess in this case), then the coalescence of the coacervate droplets would take more time and water would be slowly expelled from the coacervate phase. The kinetics of formation of the coacervate phase seemed to be pH dependent and could be measured from the initial slope of the kinetics curves. In Figure 5.3, the kinetics of the growth of the coacervate phase highlighted the pH dependence of the phase separation. At pH 4.0, the phase separation was at its fastest. The strength of the electrostatic interaction was estimated by calculating the absolute value of the product of the measured zeta potentials of the WP and of the GA molecules as a function of pH. The result is also plotted in Figure 5.3. It showed that the shapes of both curves (kinetics of phase separation and zeta potential product) were similar. It could therefore be hypothesized that the kinetics of phase separation was related to the strength of the electrostatic interaction between WP and GA molecules. Thus, the stronger the electrostatic interaction was, the faster the phase separation. The phase separation and the formation of the coacervate phase arose from the formation of insoluble WP/GA complexes that concentrated into coacervate droplets of various sizes. These coacervate droplets coalesced into a phase separated layer at the bottom of the tube. If the coacervate droplets were fully charge balanced, they would coalesce faster than if some residual charges were present. As mentioned by Sanchez *et al.* (2002a), when the proteins were in insufficient quantity, they could not totally compensate the negative charges of the GA. As a result, a surface layer of GA stabilized the coacervates, inhibiting the interactions between coacervate droplets. In these conditions, rearrangement of the coacervate was needed and the coacervate droplets settled very slowly. These results were confirmed in a recent work where the diffusivity of the WP and the GA within their coacervate phase was studied by the means of several techniques [Weinbreck *et al.*, 2004c]. One of the technique used was fluorescence recovery after photobleaching (FRAP) in combination with confocal scanning light microscope (CSLM). It appeared that most of the coacervate phases prepared at various pH values were rather homogeneous (with sometimes some water inclusion), except at pH 4.5 where even though some coacervate droplets were

coalescing slowly, after two days of phase separation, some non coalesced droplets were still visible.

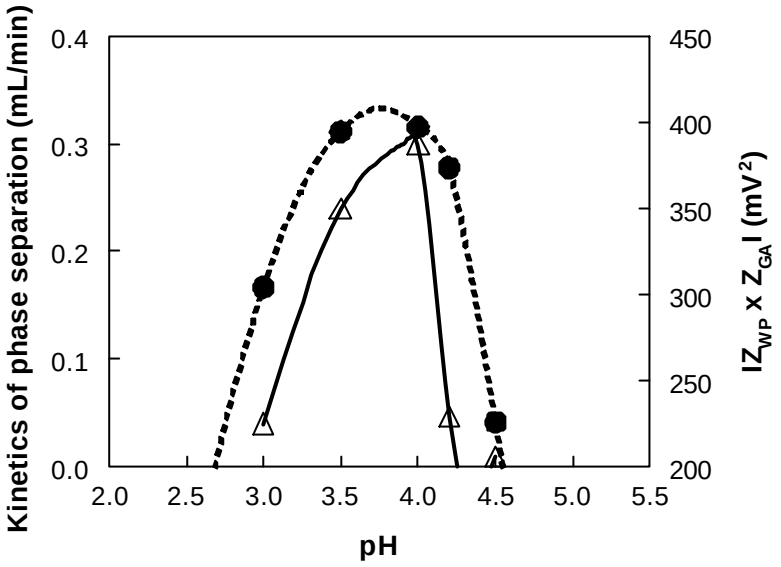

Figure 5.3: ( ): Kinetics of phase separation of WP/GA coacervate as a function of pH, Cp = 3%, $(Pr:Ps)_{ini}$ = 2:1, [NaCl] = 0 mM. ( ): Product of zetapotential of WP and GA as a function of pH.

The same experiment as above was then carried out for $(Pr:Ps)_{ini}$ = 1:1 and 8:1. The final volume (percentage of total volume) of the coacervate phase after 7 days is plotted as a function of pH in Figure 5.4. As illustrated in this figure, complex coacervation occurred in a specific pH range depending on the $(Pr:Ps)_{ini}$ ratio. For pH values close to the iso-electric point of the WP (pI = 5.2) and close to the pH at which GA became neutral (pH = 2.0), no coacervation took place because of the neutrality of one of the polymers. The maximum volume of coacervate was close to 7% of the total volume of the solution. This result was in good agreement with previous work of Burgess and Carless (1984), who reported a maximum (gelatin/GA) coacervate phase volume corresponding to 8% of the total volume. The pH at which the maximum volume of coacervate was obtained ($pH_{Vol\text{-}max}$) increased when $(Pr:Ps)_{ini}$ increased. Indeed, for a $(Pr:Ps)_{ini}$ = 8:1, $pH_{Vol\text{-}max}$ = 4.8, whereas $pH_{Vol\text{-}max}$ was between 4.0 and 4.2 for $(Pr:Ps)_{ini}$ =2:1, and between 3.0 and 3.5 for $(Pr:Ps)_{ini}$ = 1:1. This shift of $pH_{Vol\text{-}max}$ to lower values when the $(Pr:Ps)_{ini}$ decreased was understandable since fewer protein molecules were available per polysaccharide chain and a more acidic pH was

necessary to get more positive charges on the WP, which would then be sufficient to compensate the negative charges of the GA. Furthermore, the final volume of coacervate was smaller at $(Pr:Ps)_{ini}$ = 8:1 than at $(Pr:Ps)_{ini}$ = 2:1 and 1:1. This phenomenon could easily be understood, since at $(Pr:Ps)_{ini}$ = 8:1, the concentration of GA was lower than at the other ratios (same Cp but higher Pr:Ps). The voluminosity of the coacervate phase was mainly due to the voluminosty of the GA (which is a larger molecule than the WP molecules). These results were in agreement with previous studies, where Sanchez *et al.* (2002a) mentioned that changing the â-lg to GA ratio (from 1:1 to 2:1) altered the coarsening kinetics as well as the structure and morphology of coacervates.

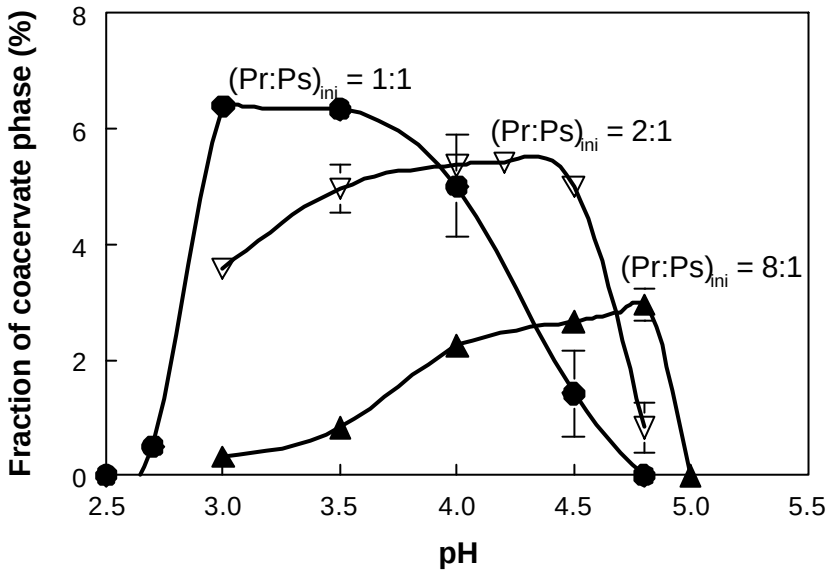

Figure 5.4: Fraction of WP/GA coacervate phase (% of total volume) as a function of pH after 7 days of phase separation. ( ): $(Pr:Ps)_{ini}$ = 1:1; (∇): $(Pr:Ps)_{ini}$ = 2:1; ( ): $(Pr:Ps)_{ini}$ = 8:1.

Composition of the coacervate phase after 48h of phase separation

Effect of pH and Pr:Ps ratio

After 48h of phase separation, the amount of water contained in the coacervate phase was measured by weighing the coacervate before and after freeze-drying. From this measurement, the total biopolymer concentration (Cp) in the WP/GA coacervates could be deduced, and it is plotted in Figure 5.5a. All the coacervates were very concentrated

in biopolymer, Cp varying from 11% (w/w) up to 33% (w/w). The results indicated that, for each $(Pr:Ps)_{ini}$, there was a pH at which the Cp was the largest ($pH_{Cp\text{-}max}$). On either side of the $pH_{Cp\text{-}max}$, Cp decreased, highlighting that fewer polymers were involved in the complex formation. Thus, at $pH_{Cp\text{-}max}$, the optimum conditions for coacervation were reached. For $(Pr:Ps)_{ini}$ = 1:1, the $pH_{Cp\text{-}max}$ = 3.5, for $(Pr:Ps)_{ini}$ = 2:1, $pH_{Cp\text{-}max}$ = 4.0, and for $(Pr:Ps)_{ini}$ = 8:1, $pH_{Cp\text{-}max}$ = 4.5. The values of the $pH_{Cp\text{-}max}$ shifted to lower values when the $(Pr:Ps)_{ini}$ was reduced. The explanation of this phenomenon was the same as described above. Indeed, by decreasing the amount of WP available per GA chain, the pH at which charge compensation occurs shifted to lower pH values, at which the WP became sufficiently charged. It is important to note that the $pH_{Vol\text{-}max}$ corresponded to the $pH_{Cp\text{-}max}$, meaning that at the optimum pH of coacervation, a large volume of highly concentrated polymers was obtained. It seemed that if more biopolymers were present in the mixture, the volume of the coacervate phase was also increased. For $(Pr:Ps)_{ini}$ = 2:1, both biopolymer concentration and coacervate volume were maximum at pH = 4.0. Furthermore, as depicted in Figure 5.3, for $(Pr:Ps)_{ini}$ = 2:1, pH 4.0 was also the pH at which the fastest kinetics of phase separation was obtained, like the pH of the maximum strength of electrostatic interaction.

From HPLC measurements carried out on the dilute upper phase of the WP/GA mixtures, the residual amount of unbound WP and GA could be determined. From this value, the ratio of WP and GA (Pr:Ps) in the coacervate phase could be calculated by taking into account the volume of the coacervate phase. The results are presented in Figure 5.5b for various $(Pr:Ps)_{ini}$ (*i.e.* 1:1, 2:1, 8:1) as a function of pH. The general trend was similar for all $(Pr:Ps)_{ini}$ studied. Increasing pH led to an increase of the Pr:Ps in the coacervate phase. This result could easily be understood by considering the charge density of the WP and the GA. Indeed, the zetapotential of WP is obviously strongly pH-dependent, and since GA is a weak polyelectrolyte, its zetapotential decreased in the pH window studied ($Z_{GA\ pH5}$ = -28 mV; $Z_{GA\ pH3.5}$ = -17 mV; $Z_{GA\ pH2}$ = 0 mV). By calculating the zeta potential ratio between WP and GA (Z_{WP}:Z_{GA}) as a function of pH, it was clear that more proteins were needed at higher pH to compensate the negative charges of the GA. At acidic pH, the WP became more charged and the GA less charged, which would explain that fewer proteins were necessary to compensate the charges of the carboxylic groups of the GA. For $(Pr:Ps)_{ini}$ = 1:1, GA was in excess in the upper phase, and for $(Pr:Ps)_{ini}$ = 8:1, WP was in excess. At $pH_{Cp\text{-}max}$, the Pr:Ps in the coacervate phase were rather similar to their respective $(Pr:Ps)_{ini}$ of 1:1 and 2:1. For

$(Pr:Ps)_{ini}$ = 8:1, the Pr:Ps ratio in the coacervate phase was 4:1 at $pH_{Cp\text{-}max}$ = 4.5. Since the kinetics of phase separation was slow as compared to the other ratio it is possible that the equilibrium was not yet obtained for this ratio. Furthermore, the surprising result lay in the observed difference of the final values of Pr:Ps in the coacervate depending on the $(Pr:Ps)_{ini}$. This result was unexpected since if the complexes were charge balanced at each pH, the amount of WP bound per GA would not be dependent on the initial Pr:Ps ratio. And here, the higher the $(Pr:Ps)_{ini}$, the higher the Pr:Ps in the coacervate phase. This result was already found by Schmitt *et al.* (1999) for a system of pure â-lg and GA. It appeared that there was still a mass action effect which led to the phase separation of more WP if the initial WP concentration was larger. Therefore, one could conclude that there was a charge adjustment of the polymers, where the pK of dissociation of the charged groups would shift to maintain the overall charge balance of the system. Thus, it seemed that the coacervate is a very flexible system that adapts to external parameters, by shifting its charge distribution and / or its chain conformation. This finding supports the fact that, when charge compensation was not instantaneously obtained, the coacervate droplets rearranged by adjusting their charges to form a charge balanced coacervate phase.

Effect of pH and ionic strength

A way to weaken the electrostatic interaction is addition of NaCl to the mixture. The increase of the ionic strength reduces the pH range where complex coacervation takes place, and above a critical [NaCl], complex coacervation is suppressed [Weinbreck *et al.*, 2003a]. The influence of the ionic strength was studied as a function of pH for a mixture of WP/GA with a $(Pr:Ps)_{ini}$ = 2:1 at pH 4.0 (these conditions were chosen since it was found that they correspond to the optimum coacervation conditions). Increasing amounts of NaCl were added to the mixture, ranging from 0 mM to 100 mM. The final volume of the coacervate phase obtained after 48 h of phase separation is plotted in Figure 5.6 together with the final Cp in the coacervate (determined from water content as described above). The results showed that increasing ionic strength led to a decrease of the coacervate volume, and above 60 mM of NaCl, no coacervate phase was obtained: coacervation was inhibited. It is also worth noting that the kinetics of phase separation decreased upon salt addition (not shown here). The Pr:Ps in the coacervate phase (determined by HPLC) remained constant, independent of the ionic strength. Furthermore, addition of NaCl led to a more watery coacervate phase, less

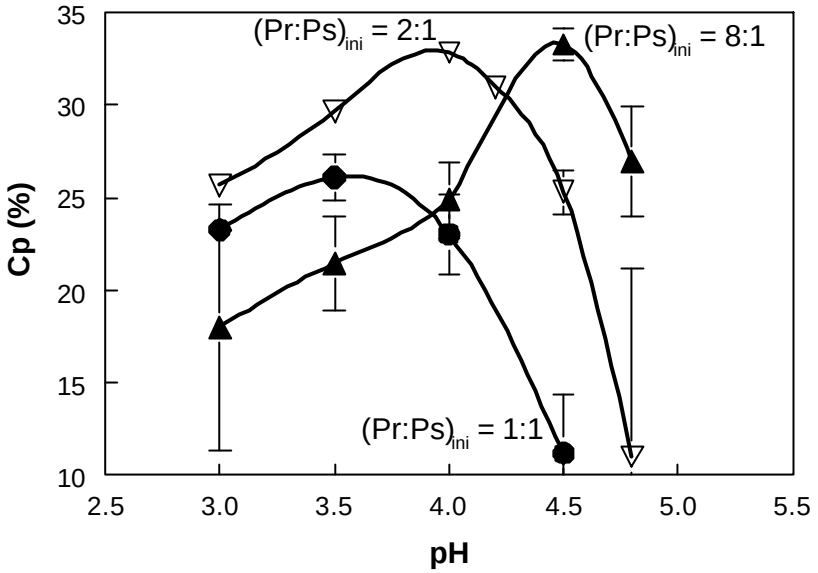

Figure 5.5a: Total biopolymer concentration (Cp) in the WP/GA coacervate phase as a function of pH after 48h of phase separation. ( ): $(Pr:Ps)_{ini}$ = 1:1; (∇): $(Pr:Ps)_{ini}$ = 2:1; ( ): $(Pr:Ps)_{ini}$ = 8:1.

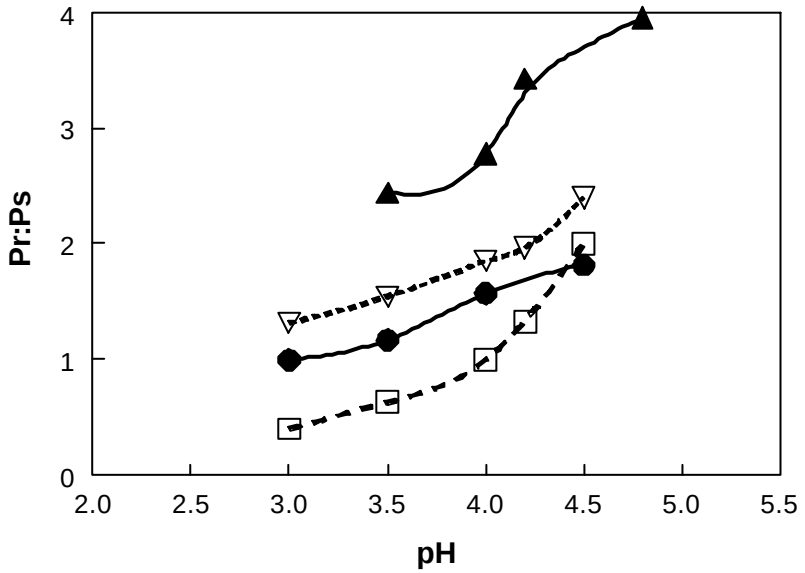

Figure 5.5b: Same system as in Figure 5.5a. Final Pr:Ps in the WP/GA coacervate phase as a function of pH after 48h of phase separation. ( ): $(Pr:Ps)_{ini}$ = 1:1; (∇): $(Pr:Ps)_{ini}$ = 2:1; ( ): $(Pr:Ps)_{ini}$ = 8:1; ( ): Zetapotential of WP / Zetapotential of GA (Z_{WP}:Z_{GA}).

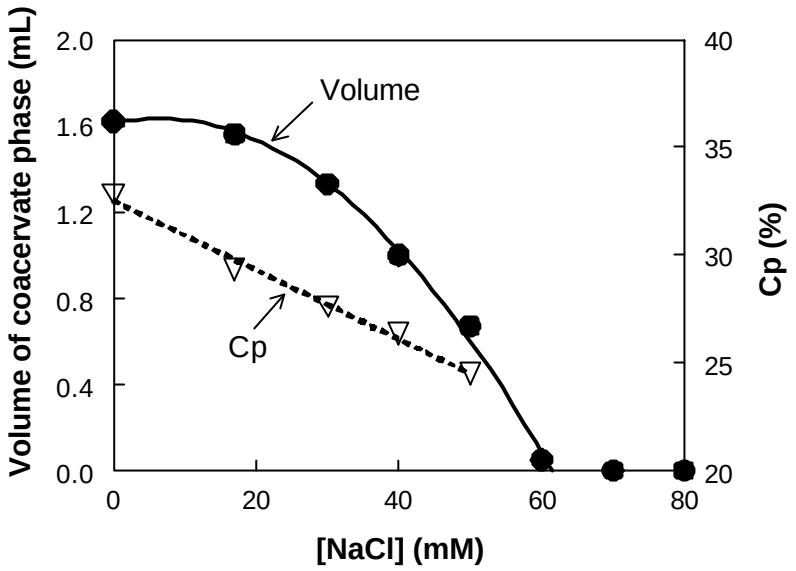

Figure 5.6: Composition of WP/GA coacervate phase as a function of the ionic strength after 48h of phase separation, $(Pr:Ps)_{ini}$ = 2:1, pH = 4.0. ( ): volume of the coacervate phase; (∇): total biopolymer concentration (Cp) in the coacervate phase.

concentrated in polymer, as described by the linear decrease of Cp as a function of [NaCl]. These results highlighted once more that the addition of microions in the mixture screened the charges of the polymers and decreased the complex formation [Bungenberg de Jong, 1949a; Weinbreck *et al.*, 2003a]. As described in the theory of Overbeek and Voorn (1957), below a critical salt concentration and a critical initial polymer concentration, the mixtures demixed into a polymer-rich phase and an aqueous phase poor in polymers. The composition of the two phases became closer when the concentration of microions was increased and finally reached a critical point, beyond which phase separation no longer occurred. As illustrated in Figure 5.6, the concentration of polymer in the coacervate phase decreased upon increasing the [NaCl]. The critical salt concentration was 60 mM in this case, which led to a critical Cp of 22%. Thus, if WP and GA were mixed at an initial Cp > 22%, no phase separation would occur. This experiment was already carried out in a previous study, where a phase diagram of mixtures of WP/GA was determined for Pr:Ps = 2:1 and at pH 3.5 [Weinbreck *et al.*, 2003a]. At pH = 3.5, the critical concentration was measured at 15% of WP and GA (Pr:Ps = 2:1). Here, the experiments were carried out at pH 4.0, the pH

at which the strongest electrostatic interactions took place; thus the critical concentration would be expected to be somewhat higher.

Small angle X-ray scattering (SAXS) measurements

Effect of pH

WP/GA coacervates were collected at various pH values as described above. Small angle X-ray scattering (SAXS) measurements were performed on each coacervate phase (fixed pH, fixed $(Pr:Ps)_{ini}$ ratio). The scattering pattern was represented by plotting the product of the scattered intensity and the wave vector (I(Q) x Q) versus the scattering wave vector Q (Holtzer plot).

Figure 5.7a shows the pattern of coacervate phases prepared at $(Pr:Ps)_{ini}$ = 2:1 and at various pH values (3.0, 3.5, 4.0, 4.2, 4.5). The scattering intensity of the initial mixture at pH 7.0 (before coacervation took place) was low and rather flat compared to the coacervated samples because of a lower polymer concentration and the absence of phase separation. The low and flat scattering pattern of the initial mixture highlighted that the system was not structured at pH 7.0. On the contrary, the scattering patterns of the coacervate phases presented characteristics features. Comparing the values of the scattered intensity in Figure 5.7a showed that the intensity decreased in the order: pH 4.5, pH 3.0, pH 3.5, pH 4.2, and pH 4.0 (c.f. inset). In Figure 5.7b the scattering patterns of the coacervate were shifted in order to compare their shapes more easily. A peak was measured at Q ~ 0.3 nm^{-1} for all the coacervate samples. The peak in the scattering pattern at Q ~ 0.3 nm^{-1} was attributed to the presence of GA. Indeed, when a (weak) polyelectrolyte like GA is present in a mixture, a peak appears corresponding to the repulsion between the charged groups of the molecule. This assumption is backed up by previous neutron scattering experiments of a GA mixture which showed a similar scattering behavior with a peak at Q = 0.2 nm-1. By increasing the ionic strength, the polyelectrolyte peak was reduced due to the screening of the carboxylic groups [unpublished result]. At pH 4.0 the concentration of GA in the coacervate phase was higher than at pH 4.2 and 4.5, as illustrated in Figure 5.5a and 5.5b, and a shift of the polyelectrolyte peak was noticeable from Q = 0.30 nm^{-1} at pH 4.5 (lower [GA]) to Q = 0.37 nm^{-1} at pH 4.0 (c.f. inset). This result was in good agreement with what one would expect for a polyelectrolyte solution. A shoulder at Q = 0.7 nm^{-1} was more or less pronounced depending on the pH value of the coacervate phase. It could be attributed

to a distribution of the WP structurally arranged in a compact manner. The position of the maximum of the shoulder was indeed independent of the WP concentration and of the pH, indicating an excluded volume type of interaction. The shoulder was the most pronounced at pH 4.0 and 4.2 (pH of maximum interaction). For pH 3.0 and 3.5, the peak faded away. This result suggested that at pH 4.0 and 4.2, the coacervate phase was more structured, thus inducing a stronger correlation between the WP molecules. To confirm this hypothesis, an attempt was made to use model calculations to predict the scattering intensity behavior of a WP/GA mixture and check whether the presence of the two peaks were really due to the GA molecules at Q ~ 0.3 nm^{-1} and WP molecules at Q = 0.7 nm^{-1}. The scattering pattern of a WP / GA mixture was calculated from the individual scattering patterns of each biopolymer. The form factor P(Q) of GA was approximated by calculating the scattering function of a charged polymer chain with excluded volume of the segments [Poetschke *et al.*, 2000]. WP are mainly composed of â-lg. The hard sphere model (radius of â-lg = 3 nm) was used to calculate the form factor P(Q) and the structure factor S(Q) of the â-lg [McQuarrie, 1973]. This approximation was very simplified but the main features of the scattering pattern were recovered. In this model, it was hypothesized that the scattering patterns of the WP and GA were independent of each other. The scattering curve model of the coacervate was therefore obtained by adding the scattering intensities calculated for â-lg and GA in the proportion as present in the coacervate phase at pH 4.0: 1.85 â-lg per 1 GA. The model calculation was compared to the experimental data in Figure 5.7c for a coacervate at pH 4.0 and showed the qualitative features of the experimental data, especially for the position of the a peak at Q = 0.7 nm^{-1}, corresponding to the structure factor of the protein, which confirmed the distribution of the WP as in a hard sphere liquid (*i.e.* WP distributed in a compact manner). Thus, one could tentatively conclude that WP served as macroions that controlled the degree of swelling of the GA molecules, especially at pH = 4.0. If the pH was decreased, the WP molecules were less numerous in the coacervate and the correlation peak was less pronounced (shoulder at Q = 0.7 nm^{-1} less pronounced) and if the electrostatic force was reduced (at pH < 4.0 or pH > 4.0), the GA molecules were less compact (peak shifting from 0.37 to 0.30 nm^{-1}), leading to a more open structure of the coacervate phase.

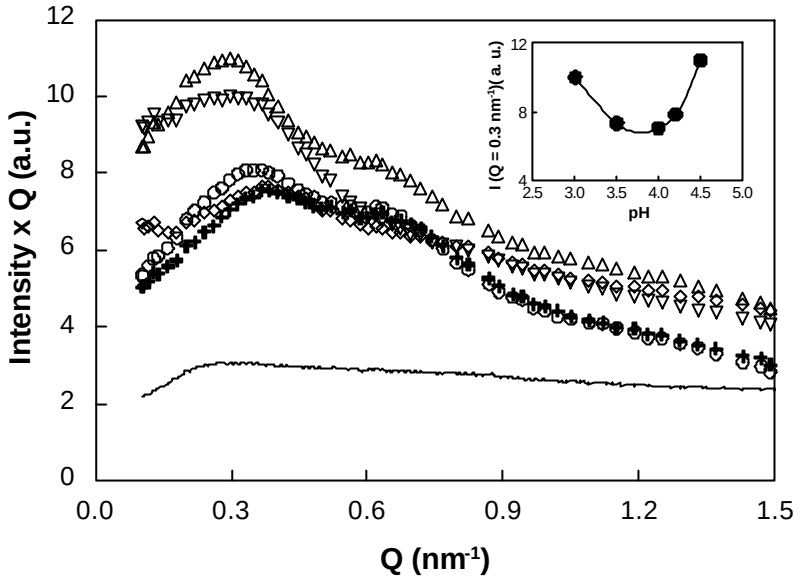

Figure 5.7a: SAXS data of WP/GA coacervate phase, $(Pr:Ps)_{ini}$ = 2:1. ( ): pH 4.5; ( ): pH 4.2; (+): pH 4.0; ( ): pH 3.5; (▽): pH 3.0; ( ): mixture of 3% WP/GA at pH 7.0. In the inset, the value of the scattering intensity at Q = 0.3 nm^{-1} is plotted as a function of pH.

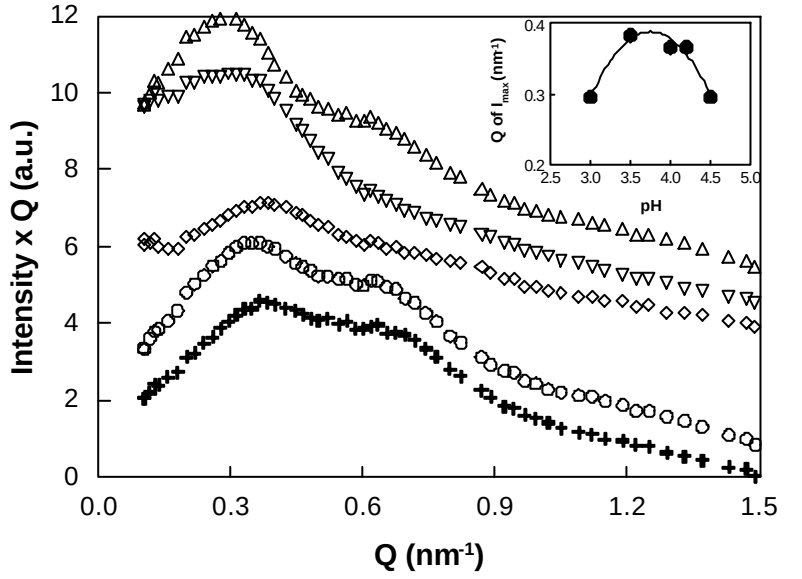

Figure 5.7b: SAXS data of WP/GA coacervate phase, $(Pr:Ps)_{ini}$ = 2:1. Same values as Figure 5.7a, but shifted for better clarity. ( ): pH 4.5; ( ): pH 4.2; (+): pH 4.0; ( ): pH 3.5; (▽): pH 3.0. In the inset, the Q value corresponding to the maximum intensity is plotted as a function of pH.

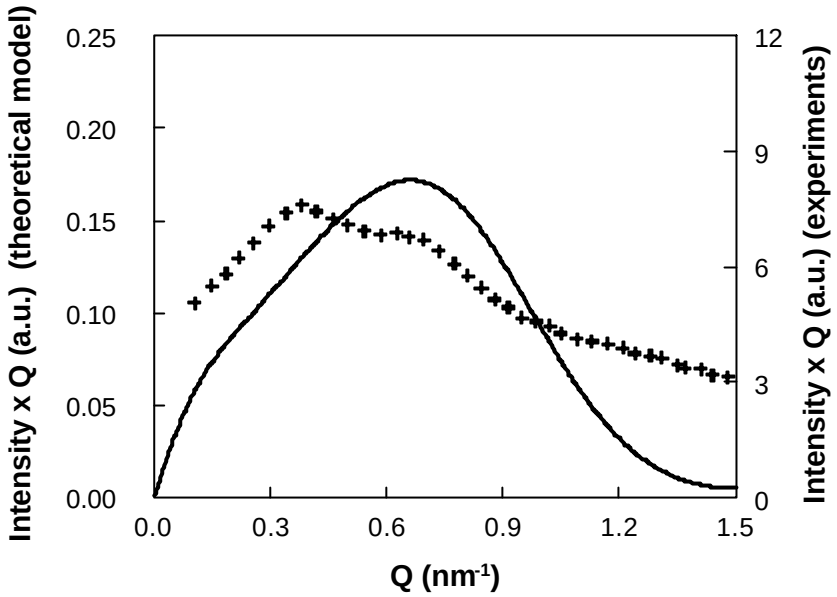

Figure 5.7c: (+): SAXS data of WP/GA coacervate, $(Pr:Ps)_{ini}$ = 2:1, pH 4.0; ( ): Theoretical calculation.

Effect of Pr:Ps

SAXS measurements were carried out on coacervates prepared at $(Pr:Ps)_{ini}$ = 1:1, 2:1 and 8:1 for various pH values. The scattering patterns of coacervate prepared at pH 4.0 for the three different $(Pr:Ps)_{ini}$ values is shown in Figure 5.8. For all the $(Pr:Ps)_{ini}$ values studied, a peak was measured at Q = 0.7 nm^{-1}, corresponding to the specific length scale in the WP distribution. The height of the polyelectrolyte peak at Q around 0.3 nm^{-1} decreased by increasing $(Pr:Ps)_{ini}$. Indeed, the amount of WP in the coacervate phase increased by increasing $(Pr:Ps)_{ini}$ as depicted in Figure 5.5b, and thus WP molecules might act as a screener of the polyelectrolyte interaction, reducing the intensity of the polyelectrolyte charge correlation peak. The scattering patterns were also compared for the three $(Pr:Ps)_{ini}$ values but at the $pH_{Cp\text{-}max}$ determined in Figure 5.5a. The results are presented in Figure 5.9. The scattering patterns followed the expected trend. The amount of GA in the coacervate phase was maximum at $(Pr:Ps)_{ini}$ = 1:1 (cf. Figures 5.5a and 5.5b). The peak at Q = 0.3 nm^{-1} was thus more pronounced for $(Pr:Ps)_{ini}$ = 1:1. The amount of WP being maximum for $(Pr:Ps)_{ini}$ = 8:1, the peak at Q = 0.7 nm^{-1} was more pronounced at this ratio. Overall, the scattering patterns depicted in Figure 5.9 were more similar to each other than the scattering patterns in Figure 5.8, showing that the structures of the coacervate were comparable at their optimum pH.

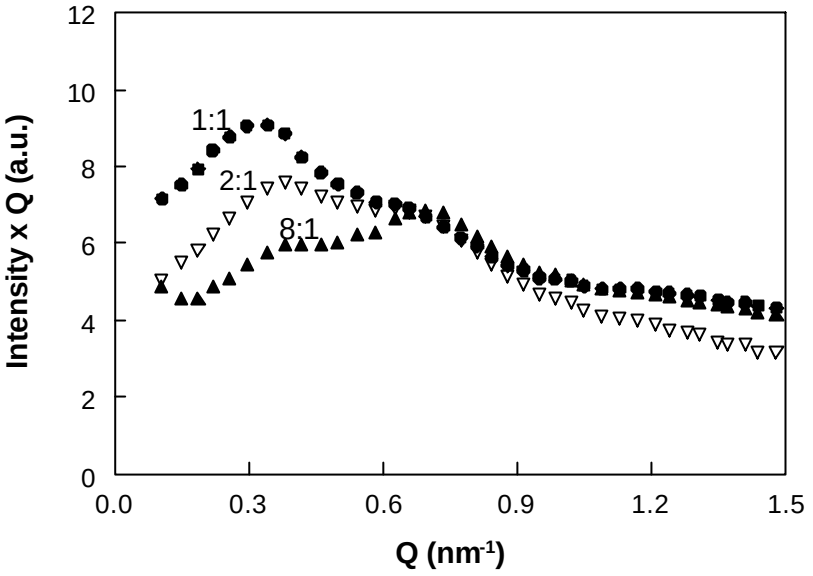

Figure 5.8: SAXS data of WP/GA coacervate phase, pH 4.0. ( ): $(Pr:Ps)_{ini}$ = 1:1; (∇): $(Pr:Ps)_{ini}$ = 2:1; ( ): $(Pr:Ps)_{ini}$ = 8:1.

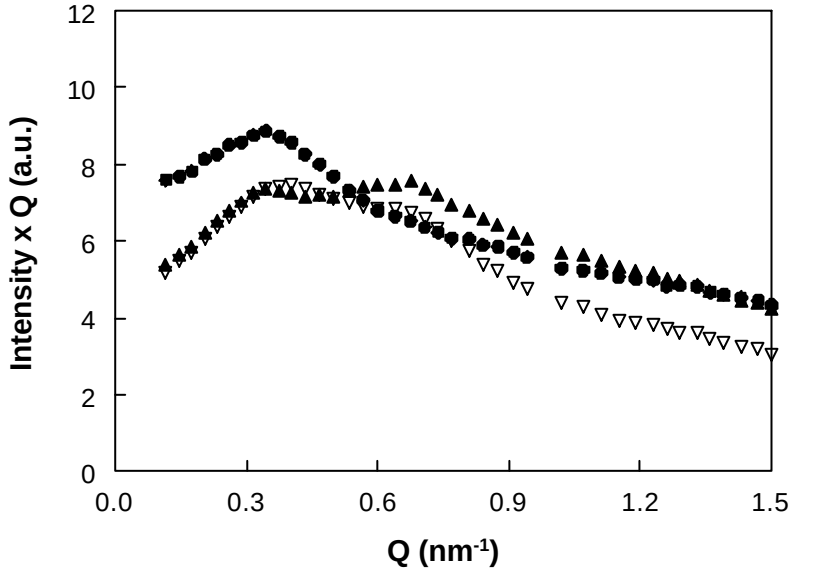

Figure 5.9: SAXS data of WP/GA coacervate phase, $pH_{Cp\text{-}max}$. ( ): $(Pr:Ps)_{ini}$ = 1:1, $pH_{Cp\text{-}max}$ = 3.5; (∇): $(Pr:Ps)_{ini}$ = 2:1, $pH_{Cp\text{-}max}$ = 4.0; ( ): $(Pr:Ps)_{ini}$ = 8:1, $pH_{Cp\text{-}max}$ = 4.5.

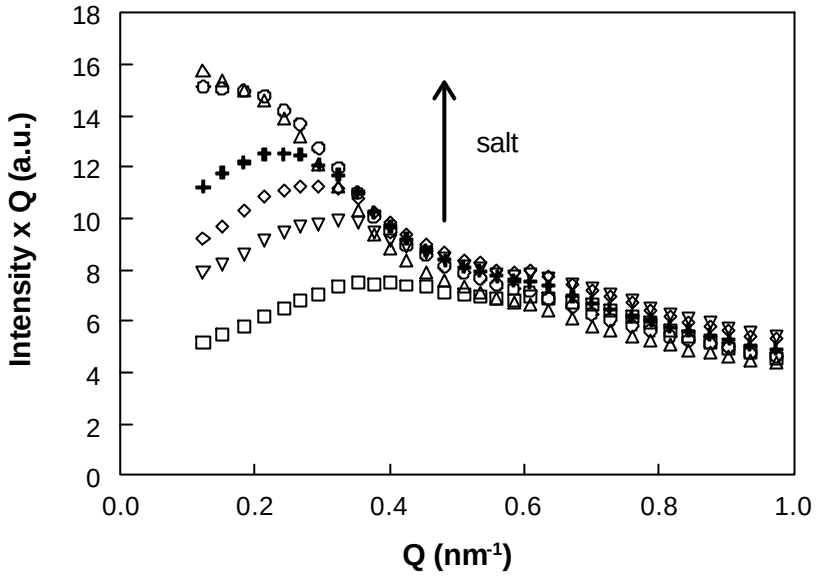

Figure 5.10a: SAXS data of WP/GA coacervate phase, $(Pr:Ps)_{ini}$ = 2:1, pH 4.0, various [NaCl]. ( ): 55 mM; ( ): 50 mM; (+): 40 mM; ( ): 30 mM; (∇): 20 mM; ( ): 0 mM.

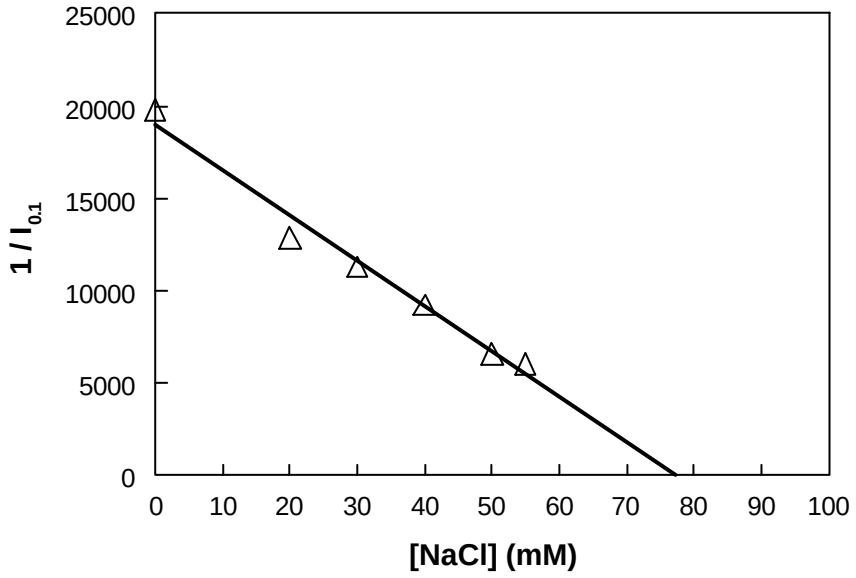

Figure 5.10b: $1/I_{0.1}$ versus [NaCl]. $I_{0.1}$ was measured from plot 9a.

Effect of the ionic strength

WP/GA coacervates were prepared at $(Pr:Ps)_{ini}$ = 2:1 at pH 4.0, and at various ionic strengths (ranging from [NaCl] = 0 mM – 55 mM). SAXS measurements were carried out on the coacervate phase and the scattering patterns are presented in Figure 5.10a. The results indicated that the addition of salt increased the scattered intensity, despite the fact that the polymer concentration decreased. When the ionic strength was increased, the strength of electrostatic interaction decreased as explained in the previous section. The structure of the coacervate also changed; the coacervate phase became less structured. By increasing [NaCl], the position of the polyelectrolyte peak moved towards lower Q values and its intensity increased, indicating a more heterogeneous and more open coacervate structure. The scattering intensity at Q = 0 nm^{-1} is proportional to the osmotic compressibility of the system [McQuarrie, 1973]. Closer to the critical point, the osmotic compressibility tends to infinity. Experimentally, the values at Q = 0 nm^{-1} were not measurable, so the inverse of the scattering intensity at Q = 0.1 nm^{-1} ($1/I_{0.1}$) is plotted as a function of NaCl concentration in Figure 5.10b. The system was moved closer to the critical point when the ionic strength was increased [Weinbreck *et al.*, 2003a]. Therefore, the compressibility was increased, as indicated by the decrease of the term $1/I_{0.1}$. The extrapolation of $1/I_{0.1}$ = 0 (corresponding to the critical point) gave a value of [NaCl] = 77 mM, which could be interpreted as the critical NaCl concentration above which no complexation occurred. In Figure 5.6, it was found that coacervation was inhibited at [NaCl] = 60 mM. Considering the rough approximation of $I_{0.1}$ as the compressibility under equilibrium, the agreement was fair.

CONCLUSIONS

The formation of complex coacervates was optimum at a specific pH value. For a $(Pr:Ps)_{ini}$ = 2:1, the optimum pH (pH_{opt}) was pH 4.0. At this particular pH, where the strength of the interaction was maximum, the volume and the density of coacervate phase were also the highest (Figures 5.4 and 5.5a) and phase separation occurred the fastest (Figure 5.3). SAXS data confirmed that, at pH_{opt}, the coacervate was dense and structured, as depicted in Figure 5.7a. From model calculation, a typical size of WP of 3 nm induced a peak at Q = 0.7 nm^{-1}, meaning that WP behaved as in a hard sphere liquid in the coacervate phase. The structure of the coacervate phase should be seen

as a network of compact GA molecules whose degree of shrinkage depended on the amount of electrostatically bound WP. When the pH was decreased, fewer protein molecules were included in the coacervate phase and the correlation peak at Q = 0.7 nm^{-1} was almost undetectable, GA molecules were less compact and the coacervate less structured. Varying $(Pr:Ps)_{ini}$ shifted the pH_{opt} to higher values when $(Pr:Ps)_{ini}$ was increased and to lower values when $(Pr:Ps)_{ini}$ was decreased. This phenomenon was due to the level of charge balance between WP and GA, which controlled the kinetics of phase separation and the structure of the coacervates, as already mentioned by Sanchez *et al*. (2002a). Another way of tuning the structure of the coacervate was by increasing the ionic strength. In doing so, the electrostatic interactions were screened and the coacervates became more watery (Figure 5.6). SAXS measurements also showed that the structure of coacervates was more heterogeneous and less structured when salt was added to the system, *i.e.* closer to the critical point (Figure 5.10a and 5.10b).

Denser or more open structures of WP/GA coacervates could be obtained by changing parameters like pH, Pr:Ps, or ionic strength. The diffusion properties and the barrier properties will be very dependent on this structure, which can be very useful for using the coacervates as barriers in encapsulation applications for instance. The diffusion of WP and GA within the coacervate phase is described in Chapter 7 [Weinbreck *et al.*, 2004c].

ACKNOWLEDGMENTS

Friesland Coberco Dairy Foods (FCDF) is acknowledged for their financial support. The authors would like to thank Vincent Gervaise and Frédérique Sanzey for their experimental assistance, Ab van der Linde for his help with the Zetasizer, and Dr. Igor Bodnár for enlightening discussions. Dr. Sven Hoffmann and Dr. Wim Bras are thanked for their technical assistance at DUBBLE (ESRF, Grenoble, France). The Netherlands Organization for the Advancement of Research (NWO) is acknowledged for providing the possibility and financial support for performing measurements at DUBBLE.